Biological Psychiatry: CNNI

Review

Physiological Considerations of Functional Magnetic Resonance Imaging in Animal Models

Akira Sumiyoshi, Robin J. Keeley, and Hanbing Lu

ABSTRACT

Characterizing the nature and underlying neurobiological causes of psychiatric and neurological diseases at the circuit and network levels has remained elusive and necessitates the use of robust animal models. Noninvasive functional magnetic resonance imaging allows systems-level insight into disease phenotype in humans and animals alike, and functional neuroimaging represents an ideal platform for translational and reverse-translational research, with common measurements collected across species. Animal neuroimaging allows invasive manipulations and conveniently bypasses many limitations associated with human subjects; however, awake animal imaging introduces its own constraints to reduce motion and limit subjective stress. Anesthetics offer a viable alternative, but the pharmacodynamics, pharmacokinetics, and molecular targets of anesthetics and their effects on physiology, neural activity, and neurovascular coupling must be considered. We discuss the physiological basis of and the influence of anesthetics on neurovascular coupling. We discuss anesthetic use in functional magnetic resonance imaging and focus on an anesthetic protocol developed in our laboratory. Finally, we discuss in detail our most recent work examining the physiological basis of resting-state functional magnetic resonance imaging using this anesthetic regimen and the future directions of animal neuroimaging research. Using animal imaging in combination with cutting-edge in vivo neuromodulatory techniques is essential for causal understanding of brain function in health and disease and offers an exemplary bridge between human and animal research studies.

Keywords: AMPA, Dexmedetomidine, Functional connectivity, LFP, Resting state, VTA

https://doi.org/10.1016/j.bpsc.2018.08.002

Circuit-level and network-level understanding of neuronal activity and its causal relationship with behavior is critical to treating neuropsychiatric and neurological diseases (1,2). Noninvasive functional imaging allows systems-level insight into disease phenotype in humans (3), and functional magnetic resonance imaging (fMRI) is the primary modality of choice owing to high spatial and temporal resolution and versatile imaging methodology. As brain stimulation emerges as a useful tool to treat neurological and psychiatric disorders (4), MRI has been used to guide stimulation targets and monitor disease progression (5–7). Nevertheless, because of ethical concerns, many imaging studies in patient populations are cross-sectional, and the relationship between behavioral phenotype and functional brain readout is generally correlational. Characterizing the nature and underlying neurobiological causes of psychiatric and neurological disease at the neural circuit and network level has proven to be less than straightforward and necessitates robust animal models.

Although no animal model precisely captures human disease, behaviors that recapitulate disease symptoms can be investigated using rodent models (8). The development of genetically targeted molecular switches with transgenic rodent lines has made it possible to manipulate the activity of strictly defined cell populations in specific projection pathways (9,10) to interrogate the causal roles of specific neuronal circuits in behavior. Functional neuroimaging represents one of the few opportunities to perform true cross-species measurements: neurovascular coupling is relatively conserved across species (11), and measures of functional connectivity are similar across humans and rodents (12,13). Indeed, the central measure of fMRI, the blood oxygen level–dependent (BOLD) response, was first identified in rats (14). Furthermore, cross-species comparisons with neuroimaging are facilitated by shared analytical tools (15). Functional imaging in rodent models can be used to combine systems-level whole-brain readout with modern in vivo cell biology tools, such as chemogenetics (16,17) and optogenetics (18–20), to explore the causal roles of neural circuits on behaviors. Functional neuroimaging represents an ideal platform for translational and reverse-translational research with common measurements quantified across rodents and humans.

Animal neuroimaging allows tight environmental and genetic control, circumventing the inherent heterogeneity of human populations. Furthermore, animal studies rely on quantitative measures of physiological processes and behavior, as compared to heavily subjective measures in human populations, which can be compromised by disease state. Crucially, as mentioned, rodent neuroimaging permits the combination of invasive and noninvasive tools, including, but not limited to, behavior (21–23), electrophysiology (24–26), and optical imaging (27–29). Finally, in contrast to human studies, direct comparison of imaging output

measures and postmortem microscopy techniques are easily implemented (30).

Animal neuroimaging should ideally be conducted within a similar parameter space as human neuroimaging: awake and behaving subjects remain still, fully responsive, and nonstressed to assess task-mediated and resting measurements of brain activity and connectivity. fMRI is notoriously sensitive to subject motion and generates loud acoustic noise, and rodents do not readily comply with these stringent requirements. Efforts have been made to immobilize rodents following training to habituate the animal to the imaging environment (19,31–33), but many studies are conducted with animals under anesthesia. Anesthetics, depending on their pharmacodynamics, pharmacokinetics, and molecular targets, influence brain metabolism, affect neurovascular coupling, and alter arousal (34,35). Thus, the choice of anesthetic agents and dose is critically important (36–38).

In this review, we begin with a brief discussion of the physiological basis of neurovascular coupling. We discuss anesthetics, their influence on neurovascular coupling, and their use with fMRI. Owing to this limited scope, we focus our discussion of applications of anesthetics in fMRI to work by our research group. Finally, we discuss future directions of animal neuroimaging research. Limitations and considerations using animal MRI have been thoroughly reviewed elsewhere (39,40).

NEUROVASCULAR COUPLING AND BOLD SIGNAL

Tight neurovascular coupling is the cornerstone of using BOLD signal as a surrogate of neuronal activity (41). During periods of activation, cerebral blood flow (CBF) increases more than the oxygen demands of the brain (42). This mismatch results in an increase in oxyhemoglobin and a decrease in deoxyhemoglobin (43), which have different magnetic properties (44–46), producing the so-called BOLD signal. This physiological phenomenon, called neurovascular coupling or functional hyperemia, is the consequence of mutual interactions among three major domains: neurons, astrocytes, and vasculature (Figure 1). Increased neural activity drives functional hyperemia through direct neural inputs to the vascular system and/or through indirect astrocytic Ca^{2+} signaling (47). The relative and temporal contributions of these two pathways have been the central interest of neurovascular coupling studies and have been debated in previous reviews (48,49).

Direct inputs onto the vasculature from glutamatergic activation of pyramidal neurons results in the downstream production of nitric oxide (NO) and prostaglandins, vasoactive messengers that induce arteriole dilation. Selective pharmacological inhibition of these molecular pathways substantially decreases BOLD response in anesthetized rats (50,51). In addition to excitatory neurons, inhibitory neurons (52) and subcortical projections (53) are recruited within the neurovascular unit depending on the properties of the activated neuronal networks (54). Compared with indirect signaling, the putative direct neuronal pathway induces a rapid response and likely mediates the initial phase of neurovascular coupling (55).

The indirect pathway via astrocytic Ca^{2+} signaling is proposed to help maintain and modulate neurovascular coupling (56) and/or the tonic control of vessel tone (57). Astrocytes are ideally positioned between neuronal and vascular systems such that a subset of processes of one astrocyte contacts tens of thousands of synapses, while another subset forms end-feet on capillaries and arterioles (58). Remarkably, astrocytes express a wide variety of ion channels, receptors, transporters, and vesicles (59), allowing them to be a key player in the neurovascular unit. Cell type–specific optical recordings combined with fMRI in rodents have successfully identified the important modulatory role of astrocytes in BOLD signals (28,29). In addition, the hemoneural hypothesis has been recently proposed (60) in which changes in parenchymal vascular tone may modulate astrocytic Ca^{2+} (61) and potentially neuronal activity (62). However, the specific molecular mechanism that mediates cerebral vascular response remains incompletely understood and has been intensively researched (63–65).

INFLUENCE OF ANESTHESIA ON NEUROVASCULAR COUPLING

Neurovascular coupling changes with anesthetics, modulating individual domains of the neurovascular unit and/or inhibiting mutual interactions among domains (Figure 1). Although the precise molecular and/or physiological mechanisms of anesthetics remain unclear, prior knowledge of anesthetic effects on the rodent brain is critical for interpreting fMRI results. We review the effects of anesthetics on neural activity and the vascular system and discuss the effects of anesthetics on neurovascular coupling, with an emphasis on the compromised interaction between neuronal activity and the hemodynamic response.

General anesthetics can induce sedation, analgesia, and loss of consciousness. These effects are exerted through their actions on inhibitory gamma-aminobutyric acid (GABA) type A receptors ($GABA_AR$s), two-pore-domain K^+ channels, and *N*-methyl-D-aspartate receptors (66), affecting the balance of excitatory and inhibitory synaptic systems (67). Brain structures including the thalamus, cortex, and midbrain reticular formation mediate the sedative, hypnotic, and immobilizing actions of general anesthetics (68). For example, volatile anesthetics induce a blockade of thalamocortical activity through enhancement of synaptic and/or extrasynaptic $GABA_AR$-mediated inhibition (69). Volatile anesthetics also exert their sedative effects through strong depression of firing rates and increased $GABA_AR$-mediated inhibition through intracortical mechanisms (70). In an elegant study comparing two anesthetics, halothane and α-chloralose, Maandag *et al.* (71) demonstrated that general anesthetics affect firing of neuronal ensembles in the cortex and alter metabolism of baseline and stimulated states and modulate event-related fMRI responses.

Suppression of neuronal firing rate caused by general anesthesia induces a reduction in CBF, although the linear relationship between metabolism and blood flow still holds under anesthesia (72). In humans, propofol, an intravenously administered anesthetic, reduced glucose metabolism and CBF (73). Certain anesthetics, specifically agents with direct effects on vasculature through NO-mediated vasodilation (74), alter the relationship between metabolism and blood flow. In rats, isoflurane, a volatile anesthetic, administered at sedative doses

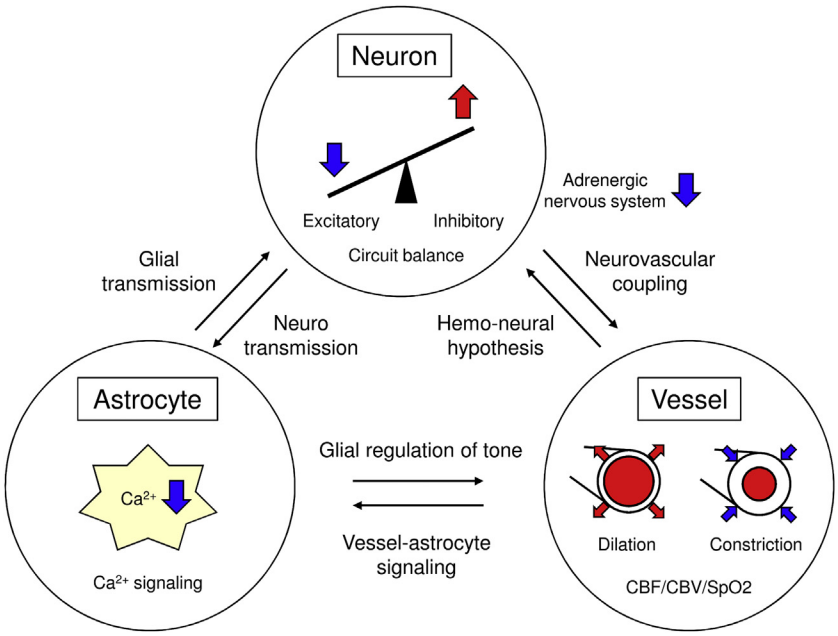

Figure 1. The effects of anesthetics on neurovascular units. The red and blue arrows indicate the identified effects of anesthetics in individual domains. The anesthetics also likely to affect the mutual interactions among domains. The blood oxygen level–dependent functional magnetic resonance imaging signal detects changes in vascular systems, but the interpretations need to consider the regulatory mechanisms of vascular systems by neurons and astrocytes. The complexity of interpretations may exist even in individual domains (neuron, excitatory vs. inhibitory; astrocyte, process vs. endfoot; vessel, artery vs. capillary or vein). CBF, cerebral blood flow; CBV, cerebral blood volume; SpO2, oxygen saturation.

profoundly decreased glucose metabolism but increased CBF (75). Following volatile anesthesia, there is a drastic increase in NO content in rat cortex (76,77). Volatile anesthetics increase CBF by inducing vasodilation via adenosine triphosphate–sensitive K^+ channels of arteriolar smooth muscle cells (78). Basal CBF under general anesthesia is of critical importance when interpreting fMRI readouts; in a human fMRI study, increased basal CBF under hypercapnia conditions (5% carbon dioxide gas mixture) increased the fMRI baseline signal and reduced the magnitude of fMRI responses to visual stimulation (79), indicating potential neurovascular uncoupling under altered basal CBF conditions.

Direct comparison of awake and anesthetized animals concomitant with observed neural activity has revealed the influence of general anesthetics on the signal transduction mechanism of neurovascular coupling (80). Over a range of stimulation conditions, the relationship between neural and hemodynamic responses is linear in awake animals, but in rats anesthetized with urethane, this relationship follows an inverted U shape (81). Urethane or isoflurane anesthesia in mice delayed and reduced hemodynamic responses to visual stimulation with no change in neural firing rate (82), which has subsequently been replicated across measurements and species (83,84). In addition, fMRI studies in humans using several anesthesia agents (isoflurane, sevoflurane, and propofol) consistently demonstrated that anesthetics decrease the intensity and extent of fMRI responses in the cortex following tactile, auditory, or visual stimulation (85). Thus, anesthetics cause disproportional changes in neural and hemodynamic responses to sensory stimulation, presumably compromising signal transduction cascades between neurons and associated vasculature.

Three mechanisms are proposed to explain this neurovascular uncoupling under anesthesia: alterations in GABAergic transmission, astrocytic Ca^{2+} signaling, and subcortical projections. First, given that specific subsets of cortical GABA interneurons are capable of dilating and constricting neighboring microvessels (52,86), general anesthetics may modulate the production of the interneuron-derived vasoactive messengers, including NO, GABA, and neuropeptides. Optogenetic fMRI research supports this proposed mechanism; direct stimulation of cortical GABAergic neurons increased CBF despite attenuating cortical spikes (87). However, the precise role of anesthetics on neurovascular uncoupling via alterations in GABAergic transmission remains unclear, and further studies are warranted. Second, doses of anesthetics (e.g., 1% isoflurane) that do not alter neuronal responses to whisker stimulation selectively suppressed astrocyte Ca^{2+} signals (88). Given that astrocytes both dilate and constrict arterioles depending on their end-feet Ca^{2+} levels (89), the suppressed hemodynamic responses under general anesthesia might be the consequences of astrocytic dysfunction. Third, the subcortical afferent projections from the locus coeruleus, raphe nucleus, and basal forebrain might play a role in cortical neurovascular coupling (90). Using fMRI and GCaMP-mediated Ca^{2+} optical fiber recordings in rats anesthetized with α-chloralose, distinct evoked astrocytic Ca^{2+} signals were coupled with positive fMRI signals, and intrinsic astrocytic Ca^{2+} signals were coupled with negative fMRI signals (28). In addition, the locus coeruleus–noradrenergic system is likely to mediate both intrinsic astrocytic Ca^{2+} signal and vasoconstriction because both were dampened in rats anesthetized with medetomidine, an alpha-2-adrenergic receptor agonist that inhibits the effect of norepinephrine on astrocytic Ca^{2+} signals (91).

fMRI IN RODENTS UNDER ANESTHESIA

Finding the best anesthetic agent that minimally affects neuronal activity and minimally interferes with neurovascular coupling has been an active pursuit in the field of animal fMRI. Since Hyder

et al. (92) reported the first fMRI experiments in α-chloralose-anesthetized rats, many anesthetics have been utilized, including urethane, propofol, isoflurane, fentanyl, halothane, pentobarbital, and nitrous oxide (93–97). Each agent has its own limitations, and none is ideal for all experimental conditions (98). Among them, isoflurane and α-chloralose have been most widely applied in the literature (99–101).

When interpreting fMRI results obtained under these two anesthesia conditions, the following factors should be carefully considered. First, α-chloralose, which is also used as a pesticide, best preserves the functional-metabolic coupling in the cortex (102), but it reduces body temperature and can produce metabolic acidosis (103), resulting in a mortality rate of 6.5% (104). Second, isoflurane decreases glucose metabolism and increases basal CBF under a sedative dose (75), blunts the hemodynamic response to sensory stimulation (105), and impairs the cerebrovascular reactivity to carbon dioxide (106). Third, α-chloralose, but not isoflurane, can alter Fos expression (107). Fourth, functional connectivity recorded with α-chloralose anesthesia moderately resembles the awake condition, but isoflurane at a dose of 1.3% results in severe differences (37). Finally, in our hands, a maximal isoflurane dose of approximately 1% is necessary for robust detection of BOLD response, yet concern remains regarding subject stress, as this dosage is insufficient to maintain prolonged immobilization.

To take advantage of the noninvasiveness of fMRI, it is often desirable to image the same animals across multiple time points and longitudinally monitor experimental manipulation effects. In 2006, Weber *et al.* (108) proposed the use of medetomidine, an alpha2-adrenergic receptor agonist, for longitudinal fMRI in rodents. They observed robust, reproducible, and significant fMRI responses similar to those obtained under α-chloralose anesthesia, likely mediated through the characteristics of medetomidine, including rapid distribution, short half-life, and the availability of an antagonist that can rapidly reverse its effects (109). While the upstream mechanism of medetomidine is known (110,111), it can cause hypertension, respiratory suppression, hyperglycemia, and bradycardia, each of which can confound the fMRI signal. Furthermore, Fukuda *et al.* (112) reported epileptic-like activity in rats sedated with medetomidine alone. The respiratory rate of rats sedated with medetomidine alone can vary substantially (35–90 breaths/min over 90 minutes) within and across animals (113). Variable arousal states and unstable physiological conditions add an additional layer of confounds to data interpretation, and stepped dose during the course of experiments has been proposed to mitigate this problem (114).

We were motivated to develop an easy-to-implement fMRI protocol that maintains consistent neurovascular coupling across longitudinal experiments. Dexmedetomidine reduces anesthetic dose requirements (115), and low doses act as both a mild sedative and an anxiolytic in rats (116) and in humans before surgical procedures (117,118). We hypothesized that combining dexmedetomidine and isoflurane would reduce dose requirements, minimizing unfavorable side effects on neurovascular coupling and BOLD response. This led us to introduce the combination of low-dose dexmedetomidine (<0.03 mg/kg/hour subcutaneously) and isoflurane (typically ≤0.5%) for longitudinal fMRI experiments in rodents. During the experiment, animals breathe spontaneously: their initial respiratory rate is approximately 40 breaths/min, gradually increases to approximately 75 breaths/min about 90 minutes following anesthesia induction, and remains stable for hours (>3 hours). During this time, arterial partial blood pressure of oxygen and carbon dioxide remain steady but slightly hypercapnic, and fMRI data are acquired during the period of stable animal physiology. Both evoked BOLD response and resting-state functional connectivity remain stable and robust during this period (119,120).

It is important to note that the exact molecular mechanisms underlying the combined effects of isoflurane and medetomidine remain unknown. Furthermore, this technique relies on spontaneous breathing and produces hypercapnia. These issues could be bypassed by artificial ventilation, which requires deep sedation, and regular blood gas sampling, both of which can introduce increased variability as well as their own set of limitations. Despite the limitations of this technique, we reported robust BOLD activation in major sensory projection pathways following unilateral naturalistic deflection of the major whiskers in rats (Figure 2), suggesting that this anesthetic protocol maintains neurovascular coupling and BOLD response. The same anesthesia protocol has also been successfully applied in rhesus monkeys, and stable and reproducible fMRI responses following odorant stimulation were reported (121). We have further applied this anesthetic regimen to resting-state fMRI scans and have discovered, defined (12), and functionally characterized (21) the rat default mode network (Figure 3); identified the network properties of the rat brain (122); and identified changes in functional connectivity measures from aging (22) and in response to drugs of abuse (23). Several studies reported frontothalamic functional connectivity in rodents under awake (123) or low-dose volatile anesthetics in rodents (124,125). However, no thalamocortical connectivity has been reported under the described anesthetic regimen for unknown reasons; this may be a direct consequence of the anesthesia.

NEUROPHYSIOLOGICAL BASIS OF RESTING-STATE fMRI SIGNAL

In disorders with prominent cognitive features, subjects often struggle or are unable to perform tasks inside the fMRI scanner. Greicius has argued that task-activation fMRI has largely failed to fulfill its promise in the clinical realm, with rare exceptions (126). Resting-state fMRI overcomes this significant limitation of task-activation MRI; instead of performing a task, subjects are instructed to rest quietly for several minutes. As resting-state fMRI scans are easy to implement in patient populations, it has been applied to study alterations in brain network functions in disease populations ranging from Alzheimer's disease (127,128) to drug addiction (129–131).

With growing applications of the resting-state fMRI technique, it is imperative to understand the neurobiological bases of the resting-state fMRI signal. This topic has attracted many laboratories using a plethora of techniques (132–137), and substantial contributions to understanding the BOLD fMRI and electrophysiological signal relationship in animal models have been described elsewhere (24,84,138,139). Despite tremendous efforts to elucidate the neural correlates of the resting-state fMRI

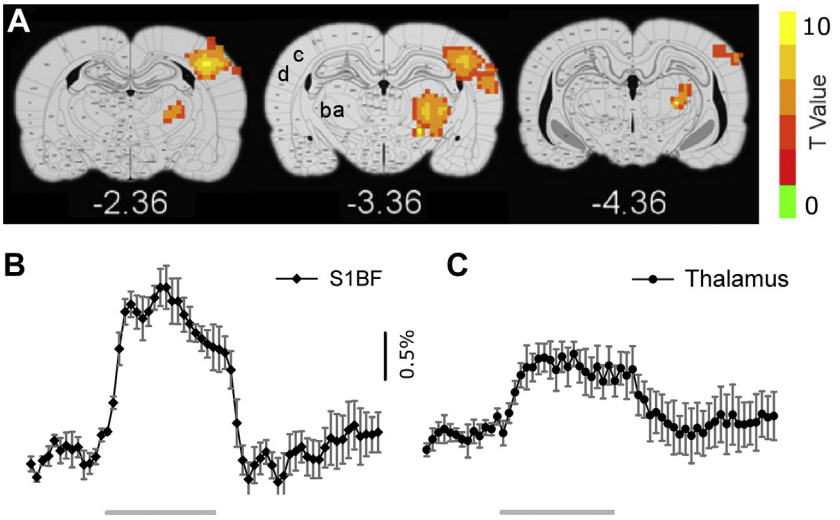

Figure 2. Functional magnetic resonance imaging response to whisker stimulation in rats. **(A)** Group activation maps (n = 9) superimposed onto rat brain atlas. Activated areas include ventromedial (a) and ventrolateral (b) thalamic nuclei, primary whisker barrel cortex (S1BF) (c), and secondary sensory cortex (d). Numbers below figures are approximate coordinates relative to rat bregma. **(B, C)** Averaged blood oxygen level–dependent responses in S1BF and thalamic nuclei across animals (n = 9, mean ± SEM). Gray lines indicated stimulus ON period, during which whiskers on the right side were deflected along the rostral-caudal direction by a comb. [Adapted with permission from Lu *et al.* (151). Copyright 2016 Proceedings of the National Academy of Sciences of the United States of America.]

signal, the neural underpinnings of specific large-scale networks remain elusive. Given that neurophysiological recording and fMRI are fundamentally different readouts of brain activity, we have argued that for the fMRI signal to be considered a surrogate for a specific neurophysiological measure, it must meet the following criteria: 1) temporal behavior of the two types of readout should be correlated across brain states; 2) correlated patterns in the signals should remain as brain state changes; 3) such patterns should distinguish one network from another; and 4) to avoid ambiguity, recordings should be made simultaneously (140). There are substantial technical challenges for an experiment to meet the above criteria.

Recently, we addressed this question by employing concurrent intracortical local field potential (LFP) recording and fMRI in rat striatum using the anesthetic regimen described above (Figure 4) (25). The striatum, critical for adaptive learning and linking motivation to behavior, is the major projection target of mesencephalic dopamine neurons and receives glutamatergic afferents from several brain regions, including the medial prefrontal cortex, hippocampus, and amygdala (141). Microinjection

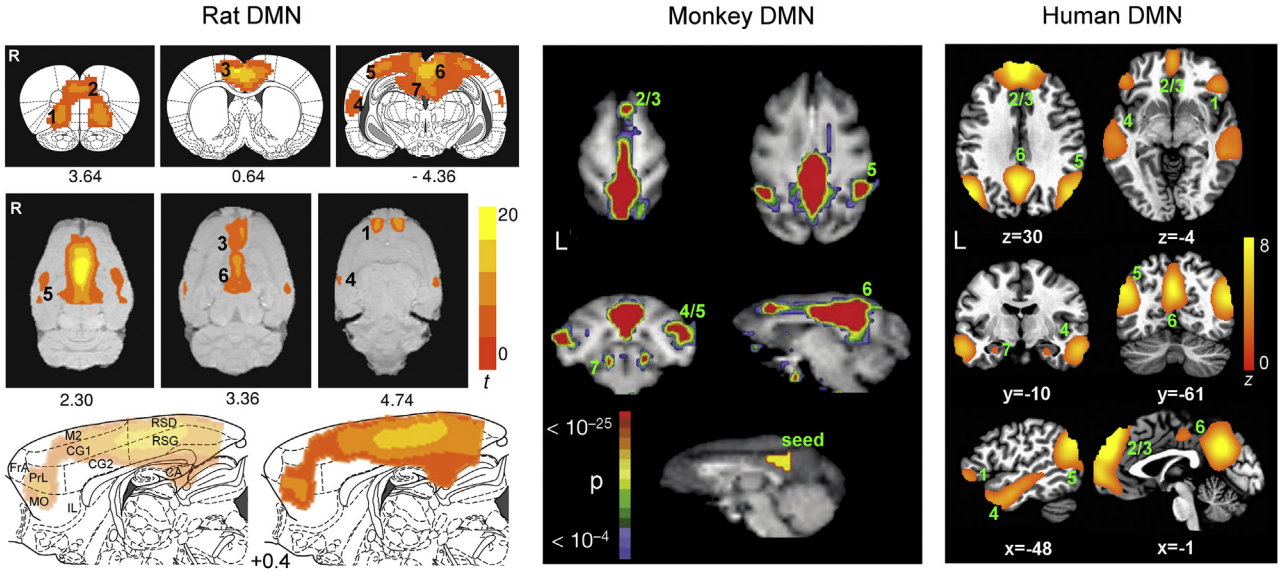

Figure 3. Comparison of the default mode network (DMN) in rat, monkey, and human. For rat DMN (left), color bar indicates t scores (n = 16, thresholded at 7 > 5.6, corrected $p < .05$). Numbers below images are approximate coordinates relative to bregma. For monkey DMN (center), the map was derived using cross-correlation method with the seed region shown. For human DMN (right), color bar indicates z scores (n = 39, thresholded at $z > 2.1$, corrected $p < .05$). CA, cornu ammonis (hippcampus); Cg1, cingulate cortex area 1; Cg2, cingulate cortex area 2; FrA, frontal association cortex; L, left; MO, medial orbital cortex; PrL, prelimbic cortex; R, right; RSD, retrosplenial dysgranular cortex; RSG, retrospenial granular cortex. [Adapted with permission from Lu *et al.* (12). Copyright 2012 Proceedings of the National Academy of Sciences of the United States of America.]

of alpha-amino-3-hydroxy-5-methyl-4-isoxazole propionic acid (AMPA), an ionotropic glutamate receptor agonist, into the ventral tegmental area enhances dopamine release in the ventral striatum (142).

We developed a concurrent fMRI–electrophysiological recording technique to perform chronic repetitive recordings with microelectrode arrays covering the striatum from its dorsolateral to ventromedial domains in combination with concurrent pharmacological modulation of striatal activity through well-defined anatomical pathways (Figure 4B). By direct application of an AMPA receptor agonist within the ventral tegmental area microcircuitry, we systematically modulated dopamine release and neuronal activity of the striatum. AMPA modulated both the amplitude and the frequency of the LFP signal (Figure 4A), and seed-based functional connectivity analysis revealed significant modulation of striatal functional connectivity by ventral tegmental area AMPA microinjection (Figure 4D–F).

To our surprise, we found a significant negative correlation between the delta (1–4 Hz) LFP and the BOLD signal, while positive correlations were observed between the beta (15–30 Hz), gamma (30–50 Hz) and high gamma (>70 Hz) LFPs and the BOLD signal (Figure 4C). Critically, regardless of the directionality in LFP-BOLD correlation across these frequency bands, the correlation maps had similar spatial patterns, covering ventral and medioventral domains of the striatum. LFP-BOLD correlations in the alpha (9–14 Hz) and theta (5–8 Hz) bands were marginally significant. This observation was unexpected but was consistent with a recent report in anesthetized monkeys by Hutchison *et al.* (143), who also reported opposite polarity in correlation between LFP band-limited power and spontaneous BOLD signal. Two major findings from this study warrant further investigation, as follows.

LFP-BOLD Correlation Is Weak

Correlations between delta LFP and the fMRI signal peaked at about −0.3, but the average was below −0.1 (Figure 4F), and the correlation between gamma LFP and the fMRI signal was similar but opposite in sign, implying that fluctuations in LFP explain only a small portion of the variance in spontaneous BOLD fluctuations. This observation is corroborated by a recent optical imaging study in awake mice (144), in which hemodynamic signals during periods of rest were weakly correlated with neural activity. Spontaneous fluctuations in cerebral blood volume (CBV) and vessel diameter persisted when local neural spiking and glutamatergic input were blocked as well as during blockade of noradrenergic receptors, suggesting a nonneuronal origin for spontaneous CBV fluctuations.

Recent optical studies reported high correlation between spontaneous CBV fluctuations and the ongoing neuronal activity detected with GCaMP sensors (145–147). The source of this discrepancy is unknown, but mouse strain (148) and definition of resting state may play a role. Specifically, if one loosely defines the resting state to be any time when the animal does not receive

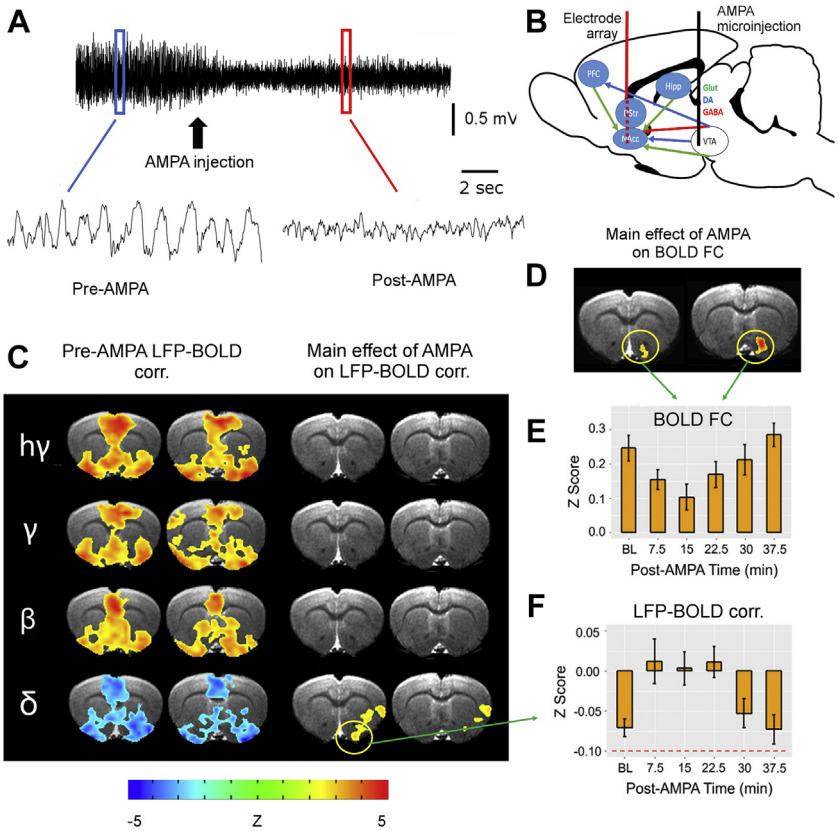

Figure 4. Magnetic resonance imaging–compatible linear electrode array was implanted into the rat striatum covering the dorsolateral and ventrolateral domains. **(A, B)** Alpha-amino-3-hydroxy-5-methyl-4-isoxazole propionic acid (AMPA) was injected into the ventral tegmental area (VTA) via a guide cannula to enhance the activity of VTA dopaminergic neurons, which project primarily to the ventral striatum, modulating striatal local field potential (LFP) signal. The waveforms before and after AMPA injection in panel **(A)** were derived from the blue and red boxes, respectively. **(C)** Effects of VTA AMPA microinjections on LFP–blood oxygen level–dependent (BOLD) correlation (corr.). All maps thresholded at $p < .05$ after correction for multiple comparisons. **(D)** Main effect of AMPA on BOLD functional connectivity (FC). **(E, F)** Time course plots of BOLD FC and LFP-BOLD correlation. Note the low correlation value in LFP-BOLD correlation, indicated by red dashed line in panel **(F)**. DA, dopamine; DSt, dorsal striatum; GABA, gamma-aminobutyric acid; Glut, glutamate; Hipp, hippocampus; NAcc, nucleus accumbens core; PFC, prefrontal cortex. [Adapted with permission from Jaime *et al.* (25).]

overt external stimulation, the correlation between spontaneous fluctuations in CBV and neural activity is high (144), similar to the results reported elsewhere (145–147). In periods when animals are still, the correlation reduced substantially.

Directionality of LFP-BOLD Correlation

The correlation between delta band LFP power and BOLD was negative in sign, while LFP power in beta and gamma band and BOLD was positive (Figure 4C), in agreement with work in monkeys (143). It remains unknown whether the directionality of the correlations was due to anesthesia or reflects a critical characteristic of the resting-state fMRI signal.

FUTURE DIRECTIONS

A summary of animal imaging studies to date is beyond the scope of this review. Despite the amount of data available, this technique is underused and represents a viable complement to the human neuroimaging literature. Translational and reverse-translational approaches to understand anesthetized versus awake conditions are sorely lacking in the current literature. Previous clinical studies reported that premedication with dexmedetomidine reduces anesthetic dose requirements for surgery, yet the pharmacological mechanisms underlying these observations are unknown. Resting-state networks and brain activation to specific task manipulation (e.g., visual or somatosenory stimulation) have been well established in humans, and isoflurane and dexmedetomidine are routinely used in the clinic. Simultaneous electroencephalography and fMRI scanning using graded anesthetic doses and comparing the results with well-established baselines (networks, task activation, and electroencephalography sleep staging) will provide a better understanding of the effects of our anesthetic regimen on neuroimaging. In addition, multimodal animal

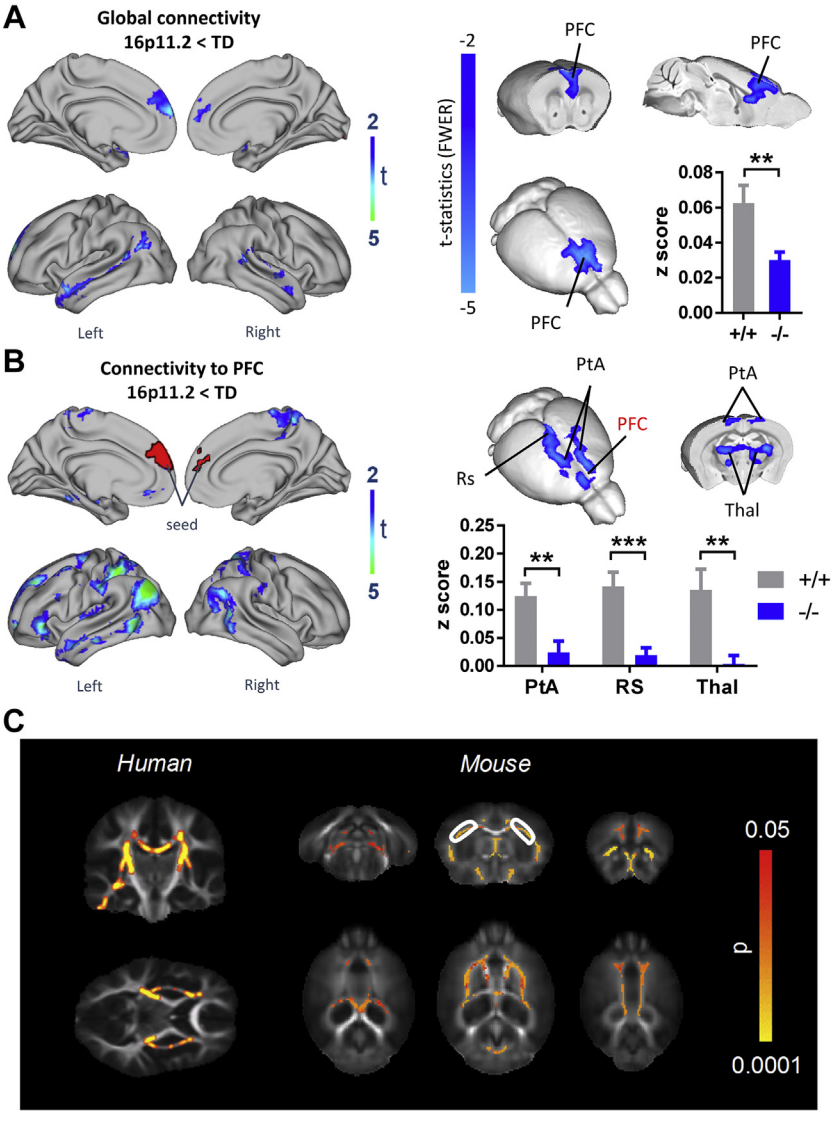

Figure 5. Autism-associated 16p11.2 microdeletion similarly impacts functional and structural connectivity in mice and humans. **(A)** Reduced global connectivity in the medial prefrontal cortex (PFC) of 16p11.2 deletion carriers compared with typically developing (TD) control subjects (left) and 16p11.2$^{+/-}$ mutant mice compared with control littermates (right). **(B)** Prefrontal cortex functional connectivity differences between 16p11.2 deletion carriers compared with typically developing control subjects (left) and 16p11.2$^{+/-}$ mutant mice compared with control littermates (right). **(C)** White matter regions with significantly increased fractional anistropy in human deletion carriers (left) and 16p11.2$^{+/-}$ mutant mice. FWER, familywise error rate; PtA, parieto-temporal areas; RS, retrosplenial cortex; Thal, thalamus. [Adapted with permission from Bertero *et al.* (124).]

imaging measuring basal perfusion, glucose consumption, and metabolites under our regimen could shed light on which brain areas and/or transmitter systems are most affected. In vivo neurochemical measurement and electrophysiology guided by imaging results could elucidate the limitations of this anesthesia regimen.

Current methods of awake animal imaging require refinement to minimize stress. A notable use of this technique involves a snuggle sack wherein rats are minimally restrained in a comfortable, non–stress-eliciting position for a narrow time window (33). Future work should use awake and actively behaving subjects without generating substantial stress. Using a head-fixed rodent that freely moved on a custom-made treadmill (149), we observed goal-directed behavior during fMRI (150). Imaging methods such as this allow behavioral mechanisms to be observed in real time and not inferred by correlating imaging measurements and scanner behaviors. Furthermore, commonalities across animal models and their associated clinical populations will provide the bridge between model organisms and clinical populations, paving the way for testing and understanding the mechanism of prevention and treatment strategies in subsequent studies. For example, using a mouse model of a specific genetic microdeletion that increases autism risk, common changes in functional and structural connectivity were observed in mice and humans (Figure 5) (124). However, beyond mechanistic understanding of disease, few studies demonstrate intervention efficacy across species. The translational and reverse-translational potential of neuroimaging has yet to be fully realized.

Animal imaging, alone or in combination with other in vivo neuromodulatory techniques, is necessary for mechanistic understanding of brain function and disease. As circuit-level and network-level causal insight into brain and behavior advances with the use of animal models, animal neuroimaging in combination with these techniques will link animal and human neuroimaging research. The wealth of information and essential data possible using animal imaging has not been fully realized, and human studies should capitalize on the work being conducted in rodents to understand and interpret cross-sectional data observed in healthy and disease populations.

ACKNOWLEDGMENTS AND DISCLOSURES

This work was supported by the Japan Society for the Promotion of Science Overseas Research Fellowships (to AS) and Canadian Institutes of Health Research Fellowship award (to RJK) and in part by the National Institutes of Health Intramural Research Program of the National Institute on Drug Abuse.

A patent pertaining to the methods and device for awake rodent imaging, of which HL is a co-inventor, has been issued to the National Institutes of Health. The remaining authors report no biomedical financial interests or potential conflicts of interest.

ARTICLE INFORMATION

From the Neuroimaging Research Branch, National Institute on Drug Abuse, National Institutes of Health, Baltimore, Maryland.

AS and RJK contributed equally to this work.

Address correspondence to Hanbing Lu, Ph.D., 251 Bayview Boulevard, Suite 200, Room 07A727, Baltimore, MD 21224; E-mail: luha@intra.nida.nih.gov.

Received Apr 19, 2018; revised Jul 31, 2018; accepted Aug 2, 2018.

REFERENCES

1. Deisseroth K, Etkin A, Malenka RC (2015): Optogenetics and the circuit dynamics of psychiatric disease. JAMA 313:2019–2020.
2. Fornito A, Zalesky A, Breakspear M (2015): The connectomics of brain disorders. Nat Rev Neurosci 16:159–172.
3. Braun U, Schaefer A, Betzel RF, Tost H, Meyer-Lindenberg A, Bassett DS (2018): From maps to multi-dimensional network mechanisms of mental disorders. Neuron 97:14–31.
4. Downar J, Blumberger DM, Daskalakis ZJ (2016): The neural crossroads of psychiatric illness: An emerging target for brain stimulation. Trends Cogn Sci (Regul Ed) 20:107–120.
5. Fox MD, Buckner RL, Liu H, Chakravarty MM, Lozano AM, Pascual-Leone A (2014): Resting-state networks link invasive and noninvasive brain stimulation across diverse psychiatric and neurological diseases. Proc Natl Acad Sci U S A 111:E4367–E4375.
6. Fitzgerald PB, Hoy K, McQueen S, Maller JJ, Herring S, Segrave R, *et al.* (2009): A randomized trial of rTMS targeted with MRI based neuro-navigation in treatment-resistant depression. Neuropsychopharmacology 34:1255–1262.
7. Drysdale AT, Grosenick L, Downar J, Dunlop K, Mansouri F, Meng Y, *et al.* (2017): Resting-state connectivity biomarkers define neurophysiological subtypes of depression. Nat Med 23:28–38.
8. Donaldson ZR, Hen R (2015): From psychiatric disorders to animal models: A bidirectional and dimensional approach. Biol Psychiatry 77:15–21.
9. Deisseroth K (2014): Circuit dynamics of adaptive and maladaptive behaviour. Nature 505:309–317.
10. Rajasethupathy P, Ferenczi E, Deisseroth K (2016): Targeting neural circuits. Cell 165:524–534.
11. de Zwart JA, Silva AC, van Gelderen P, Kellman P, Fukunaga M, Chu R, *et al.* (2005): Temporal dynamics of the BOLD fMRI impulse response. Neuroimage 24:667–677.
12. Lu H, Zou Q, Gu H, Raichle ME, Stein EA, Yang Y (2012): Rat brains also have a default mode network. Proc Natl Acad Sci U S A 109:3979–3984.
13. Pagani M, Bifone A, Gozzi A (2016): Structural covariance networks in the mouse brain. Neuroimage 129:55–63.
14. Ogawa S, Lee TM, Kay AR, Tank DW (1990): Brain magnetic resonance imaging with contrast dependent on blood oxygenation. Proc Natl Acad Sci U S A 87:9868–9872.
15. Schweinhardt P, Fransson P, Olson L, Spenger C, Andersson JLR (2003): A template for spatial normalisation of MR images of the rat brain. J Neurosci Methods 129:105–113.
16. Giorgi A, Migliarini S, Galbusera A, Maddaloni G, Mereu M, Margiani G, *et al.* (2017): Brain-wide mapping of endogenous serotonergic transmission via chemogenetic fMRI. Cell Rep 21:910–918.
17. Roelofs TJM, Verharen JPH, van Tilborg GAF, Boekhoudt L, van der Toorn A, de Jong JW, *et al.* (2017): A novel approach to map induced activation of neuronal networks using chemogenetics and functional neuroimaging in rats: A proof-of-concept study on the mesocorticolimbic system. Neuroimage 156:109–118.
18. Lee JH, Durand R, Gradinaru V, Zhang F, Goshen I, Kim D-S, *et al.* (2010): Global and local fMRI signals driven by neurons defined optogenetically by type and wiring. Nature 465:788–792.
19. Ferenczi EA, Zalocusky KA, Liston C, Grosenick L, Warden MR, Amatya D, *et al.* (2016): Prefrontal cortical regulation of brainwide circuit dynamics and reward-related behavior. Science 351:aac9698.
20. Lohani S, Poplawsky AJ, Kim SG, Moghaddam B (2017): Unexpected global impact of VTA dopamine neuron activation as measured by opto-fMRI. Mol Psychiatry 22:585–594.
21. Hsu LM, Liang X, Gu H, Brynildsen JK, Stark JA, Ash JA, *et al.* (2016): Constituents and functional implications of the rat default mode network. Proc Natl Acad Sci U S A 113:E4541–E4547.
22. Ash JA, Lu H, Taxier LR, Long JM, Yang Y, Stein EA, Rapp PR (2016): Functional connectivity with the retrosplenial cortex predicts cognitive aging in rats. Proc Natl Acad Sci U S A 113:12286–12291.
23. Lu H, Chefer S, Kurup PK, Guillem K, Vaupel DB, Ross TJ, *et al.* (2012): fMRI response in the medial prefrontal cortex predicts

cocaine but not sucrose self-administration history. Neuroimage 62:1857–1866.
24. Logothetis NK, Pauls J, Augath M, Trinath T, Oeltermann A (2001): Neurophysiological investigation of the basis of the fMRI signal. Nature 412:150–157.
25. Jaime S, Gu H, Sadacca BF, Stein EA, Cavazos JE, Yang Y, Lu H (2019): Delta rhythm orchestrates the neural activity underlying the resting state BOLD signal via phase-amplitude coupling. Cereb Cortex 29:119–133.
26. Sumiyoshi A, Riera JJ, Ogawa T, Kawashima R (2011): A mini-cap for simultaneous EEG and fMRI recording in rodents. Neuroimage 54:1951–1965.
27. Schlegel F, Sych Y, Schroeter A, Stobart J, Weber B, Helmchen F, Rudin M (2018): Fiber-optic implant for simultaneous fluorescence-based calcium recordings and BOLD fMRI in mice. Nat Protoc 13:840–855.
28. Wang M, He Y, Sejnowski TJ, Yu X (2018): Brain-state dependent astrocytic Ca2+signals are coupled to both positive and negative BOLD-fMRI signals. Proc Natl Acad Sci U S A 115:E1647–E1656.
29. Schulz K, Sydekum E, Krueppel R, Engelbrecht CJ, Schlegel F, Schröter A, *et al.* (2012): Simultaneous BOLD fMRI and fiber-optic calcium recording in rat neocortex. Nat Methods 9:597–602.
30. Gorges M, Roselli F, Müller H-P, Ludolph AC, Rasche V, Kassubek J (2017): Functional connectivity mapping in the animal model: principles and applications of resting-state fMRI. Front Neurol 8:200.
31. Martin CJ, Kennerley AJ, Berwick J, Port M, Mayhew JEW (2013): Functional MRI in conscious rats using a chronically implanted surface coil. J Magn Reson Imaging 38:739–744.
32. King JA, Garelick TS, Brevard ME, Chen W, Messenger TL, Duong TQ, Ferris CF (2005): Procedure for minimizing stress for fMRI studies in conscious rats. J Neurosci Methods 148:154–160.
33. Chang PC, Procissi D, Bao Q, Centeno MV, Baria A, Apkarian AV (2016): Novel method for functional brain imaging in awake minimally restrained rats. J Neurophysiol 116:61–80.
34. Brown EN, Purdon PL, Van Dort CJ (2011): General anesthesia and altered states of arousal: A systems neuroscience analysis. Annu Rev Neurosci 34:601–628.
35. Alkire MT, Hudetz AG, Tononi G (2008): Consciousness and anesthesia. Science 322:876–880.
36. Williams KA, Magnuson M, Majeed W, LaConte SM, Peltier SJ, Hu X, Keilholz SD (2010): Comparison of alpha-chloralose, medetomidine and isoflurane anesthesia for functional connectivity mapping in the rat. Magn Reson Imaging 28:995–1003.
37. Paasonen J, Stenroos P, Salo RA, Kiviniemi V, Gröhn O (2018): Functional connectivity under six anesthesia protocols and the awake condition in rat brain. Neuroimage 172:9–20.
38. Franceschini MA, Radhakrishnan H, Thakur K, Wu W, Ruvinskaya S, Carp S, Boas DA (2010): The effect of different anesthetics on neurovascular coupling. Neuroimage 51:1367–1377.
39. Pan WJ, Billings JCW, Grooms JK, Shakil S, Keilholz SD (2015): Considerations for resting state functional MRI and functional connectivity studies in rodents. Front Neurosci 9:269.
40. Gozzi A, Schwarz AJ (2016): Large-scale functional connectivity networks in the rodent brain. Neuroimage 127:496–509.
41. Logothetis NK, Wandell BA (2004): Interpreting the BOLD signal. Annu Rev Physiol 66:735–769.
42. Fox PT, Raichle ME (1986): Focal physiological uncoupling of cerebral blood flow and oxidative metabolism during somatosensory stimulation in human subjects. Proc Natl Acad Sci U S A 83:1140–1144.
43. Fox PT, Raichle ME, Mintun MA, Dence C (1988): Nonoxidative glucose consumption during focal physiologic neural activity. Science 241:462–464.
44. Bren KL, Eisenberg R, Gray HB (2015): Discovery of the magnetic behavior of hemoglobin: A beginning of bioinorganic chemistry. Proc Natl Acad Sci U S A 112:13123–13127.
45. Pauling L, Coryell CD (1936): The magnetic properties and structure of hemoglobin, oxyhemoglobin and carbonmonoxyhemoglobin. Proc Natl Acad Sci U S A 22:210–216.
46. Pauling L, Coryell CD (1936): The magnetic properties and structure of the hemochromogens and related substances. Proc Natl Acad Sci U S A 22:159–163.
47. Attwell D, Buchan AM, Charpak S, Lauritzen M, Macvicar BA, Newman EA (2010): Glial and neuronal control of brain blood flow. Nature 468:232–243.
48. Riera JJ, Sumiyoshi A (2010): Brain oscillations: Ideal scenery to understand the neurovascular coupling. Curr Opin Neurol 23:374–381.
49. Cauli B, Hamel E (2010): Revisiting the role of neurons in neurovascular coupling. Front Neuroenergetics 2:9.
50. Stefanovic B, Bosetti F, Silva AC (2006): Modulatory role of cyclooxygenase-2 in cerebrovascular coupling. Neuroimage 32:23–32.
51. Stefanovic B, Schwindt W, Hoehn M, Silva AC (2007): Functional uncoupling of hemodynamic from neuronal response by inhibition of neuronal nitric oxide synthase. J Cereb Blood Flow Metab 27:741–754.
52. Cauli B, Tong XK, Rancillac A, Serluca N, Lambolez B, Rossier J, Hamel E (2004): Cortical GABA interneurons in neurovascular coupling: Relays for subcortical vasoactive pathways. J Neurosci 24:8940–8949.
53. Lecrux C, Hamel E (2016): Neuronal networks and mediators of cortical neurovascular coupling responses in normal and altered brain states. Philos Trans R Soc Lond B Biol Sci 371:20150350.
54. Enager P, Piilgaard H, Offenhauser N, Kocharyan A, Fernandes P, Hamel E, Lauritzen M (2009): Pathway-specific variations in neurovascular and neurometabolic coupling in rat primary somatosensory cortex. J Cereb Blood Flow Metab 29:976–986.
55. Institoris Á, Rosenegger DG, Gordon GR (2015): Arteriole dilation to synaptic activation that is sub-threshold to astrocyte endfoot Ca2+ transients. J Cereb Blood Flow Metab 35:1411–1415.
56. Zonta M, Angulo MC, Gobbo S, Rosengarten B, Hossmann KA, Pozzan T, Carmignoto G (2003): Neuron-to-astrocyte signaling is central to the dynamic control of brain microcirculation. Nat Neurosci 6:43–50.
57. Rosenegger DG, Tran CHT, Wamsteeker Cusulin JI, Gordon GR (2015): Tonic local brain blood flow control by astrocytes independent of phasic neurovascular coupling. J Neurosci 35:13463–13474.
58. Mishra A (2017): Binaural blood flow control by astrocytes: Listening to synapses and the vasculature. J Physiol (Lond) 595:1885–1902.
59. Verkhratsky A, Nedergaard M (2018): Physiology of astroglia. Physiol Rev 98:239–389.
60. Moore CI, Cao R (2008): The hemo-neural hypothesis: On the role of blood flow in information processing. J Neurophysiol 99:2035–2047.
61. Kim KJ, Iddings JA, Stern JE, Blanco VM, Croom D, Kirov SA, Filosa JA (2015): Astrocyte contributions to flow/pressure-evoked parenchymal arteriole vasoconstriction. J Neurosci 35:8245–8257.
62. Kim KJ, Ramiro Diaz J, Iddings JA, Filosa JA (2016): Vasculo-neuronal coupling: Retrograde vascular communication to brain neurons. J Neurosci 36:12624–12639.
63. Bazargani N, Attwell D (2016): Astrocyte calcium signaling: The third wave. Nat Neurosci 19:182–189.
64. Fiacco TA, McCarthy KD (2018): Multiple lines of evidence indicate that gliotransmission does not occur under physiological conditions. J Neurosci 38:3–13.
65. Savtchouk I, Volterra A (2018): Gliotransmission: Beyond black-and-white. J Neurosci 38:14–25.
66. Franks NP (2008): General anaesthesia: From molecular targets to neuronal pathways of sleep and arousal. Nat Rev Neurosci 9:370–386.
67. Destexhe A, Rudolph M, Paré D (2003): The high-conductance state of neocortical neurons in vivo. Nat Rev Neurosci 4:739–751.
68. Rudolph U, Antkowiak B (2004): Molecular and neuronal substrates for general anaesthetics. Nat Rev Neurosci 5:709–720.
69. Jia F, Yue M, Chandra D, Homanics GE, Goldstein PA, Harrison NL (2008): Isoflurane is a potent modulator of extrasynaptic GABA(A) receptors in the thalamus. J Pharmacol Exp Ther 324:1127–1135.

70. Hentschke H, Schwarz C, Antkowiak B (2005): Neocortex is the major target of sedative concentrations of volatile anaesthetics: Strong depression of firing rates and increase of GABAA receptor-mediated inhibition. Eur J Neurosci 21:93–102.
71. Maandag NJG, Coman D, Sanganahalli BG, Herman P, Smith AJ, Blumenfeld H, *et al.* (2007): Energetics of neuronal signaling and fMRI activity. Proc Natl Acad Sci U S A 104:20546–20551.
72. Sloan TB (2002): Anesthetics and the brain. Anesthesiol Clin North Am 20:265–292.
73. Schlünzen L, Juul N, Hansen KV, Cold GE (2012): Regional cerebral blood flow and glucose metabolism during propofol anaesthesia in healthy subjects studied with positron emission tomography. Acta Anaesthesiol Scand 56:248–255.
74. Toda N, Toda H, Hatano Y (2007): Nitric oxide: Involvement in the effects of anesthetic agents. Anesthesiology 107:822–842.
75. Maekawa T, Tommasino C, Shapiro HM, Keifer-Goodman J, Kohlenberger RW (1986): Local cerebral blood flow and glucose utilization during isoflurane anesthesia in the rat. Anesthesiology 65:144–151.
76. Sjakste N, Baumane L, Meirena D, Lauberte L, Dzintare M, Kalviņs I (1999): Drastic increase in nitric oxide content in rat brain under halothane anesthesia revealed by EPR method. Biochem Pharmacol 58:1955–1959.
77. Baumane L, Dzintare M, Zvejniece L, Meirena D, Lauberte L, Sile V, *et al.* (2002): Increased synthesis of nitric oxide in rat brain cortex due to halogenated volatile anesthetics confirmed by EPR spectroscopy. Acta Anaesthesiol Scand 46:378–383.
78. Iida H, Ohata H, Iida M, Watanabe Y, Dohi S (1998): Isoflurane and sevoflurane induce vasodilation of cerebral vessels via ATP-sensitive K+ channel activation. Anesthesiology 89:954–960.
79. Cohen ER, Ugurbil K, Kim S-G (2002): Effect of basal conditions on the magnitude and dynamics of the blood oxygenation level-dependent fMRI response. J Cereb Blood Flow Metab 22:1042–1053.
80. Gao YR, Ma Y, Zhang Q, Winder AT, Liang Z, Antinori L, *et al.* (2017): Time to wake up: Studying neurovascular coupling and brain-wide circuit function in the un-anesthetized animal. Neuroimage 153:382–398.
81. Martin C, Martindale J, Berwick J, Mayhew J (2006): Investigating neural-hemodynamic coupling and the hemodynamic response function in the awake rat. Neuroimage 32:33–48.
82. Pisauro MA, Dhruv NT, Carandini M, Benucci A (2013): Fast hemodynamic responses in the visual cortex of the awake mouse. J Neurosci 33:18343–18351.
83. Aksenov DP, Li L, Miller MJ, Iordanescu G, Wyrwicz AM (2015): Effects of anesthesia on BOLD signal and neuronal activity in the somatosensory cortex. J Cereb Blood Flow Metab 35:1819–1826.
84. Goense JBM, Logothetis NK (2008): Neurophysiology of the BOLD fMRI signal in awake monkeys. Curr Biol 18:631–640.
85. MacDonald AA, Naci L, MacDonald PA, Owen AM (2015): Anesthesia and neuroimaging: Investigating the neural correlates of unconsciousness. Trends Cogn Sci (Regul Ed) 19:100–107.
86. Uhlirova H, Kılıç K, Tian P, Thunemann M, Desjardins M, Saisan PA, *et al.* (2016): Cell type specificity of neurovascular coupling in cerebral cortex. Elife 5:e14315.
87. Anenberg E, Chan AW, Xie Y, LeDue JM, Murphy TH (2015): Optogenetic stimulation of GABA neurons can decrease local neuronal activity while increasing cortical blood flow. J Cereb Blood Flow Metab 35:1579–1586.
88. Thrane AS, Rangroo Thrane V, Zeppenfeld D, Lou N, Xu Q, Nagelhus EA, Nedergaard M (2012): General anesthesia selectively disrupts astrocyte calcium signaling in the awake mouse cortex. Proc Natl Acad Sci U S A 109:18974–18979.
89. Girouard H, Bonev AD, Hannah RM, Meredith A, Aldrich RW, Nelson MT (2010): Astrocytic endfoot Ca2+ and BK channels determine both arteriolar dilation and constriction. Proc Natl Acad Sci U S A 107:3811–3816.
90. Hamel E (2006): Perivascular nerves and the regulation of cerebrovascular tone. J Appl Physiol 100:1059–1064.
91. Paukert M, Agarwal A, Cha J, Doze VA, Kang JU, Bergles DE (2014): Norepinephrine controls astroglial responsiveness to local circuit activity. Neuron 82:1263–1270.
92. Hyder F, Behar KL, Martin MA, Blamire AM, Shulman RG (1994): Dynamic magnetic resonance imaging of the rat brain during forepaw stimulation. J Cereb Blood Flow Metab 14:649–655.
93. Luo F, Xi ZX, Wu G, Liu C, Gardner EL, Li SJ (2004): Attenuation of brain response to heroin correlates with the reinstatement of heroin-seeking in rats by fMRI. Neuroimage 22:1328–1335.
94. Lahti KM, Ferris CF, Li F, Sotak CH, King JA (1999): Comparison of evoked cortical activity in conscious and propofol-anesthetized rats using functional MRI. Magn Reson Med 41:412–416.
95. Hendrich KS, Kochanek PM, Melick JA, Schiding JK, Statler KD, Williams DS, *et al.* (2001): Cerebral perfusion during anesthesia with fentanyl, isoflurane, or pentobarbital in normal rats studied by arterial spin-labeled MRI. Magn Reson Med 46:202–206.
96. Lin YJ, Koretsky AP (1997): Manganese ion enhances T1-weighted MRI during brain activation: An approach to direct imaging of brain function. Magn Reson Med 38:378–388.
97. Weng JC, Chen JH, Yang PF, Tseng WYI (2007): Functional mapping of rat barrel activation following whisker stimulation using activity-induced manganese-dependent contrast. Neuroimage 36:1179–1188.
98. Tremoleda JL, Macholl S, Sosabowski JK (2018): Anesthesia and monitoring of animals during MRI studies. Methods Mol Biol 1718:423–439.
99. Yang X, Hyder F, Shulman RG (1996): Activation of single whisker barrel in rat brain localized by functional magnetic resonance imaging. Proc Natl Acad Sci U S A 93:475–478.
100. Silva AC, Koretsky AP (2002): Laminar specificity of functional MRI onset times during somatosensory stimulation in rat. Proc Natl Acad Sci U S A 99:15182–15187.
101. Lu H, Zuo Y, Gu H, Waltz JA, Zhan W, Scholl CA, *et al.* (2007): Synchronized delta oscillations correlate with the resting-state functional MRI signal. Proc Natl Acad Sci U S A 104:18265–18269.
102. Ueki M, Mies G, Hossmann KA (1992): Effect of alpha-chloralose, halothane, pentobarbital and nitrous oxide anesthesia on metabolic coupling in somatosensory cortex of rat. Acta Anaesthesiol Scand 36:318–322.
103. Low LA, Bauer LC, Klaunberg BA (2016): Comparing the effects of isoflurane and alpha chloralose upon mouse physiology. PLoS One 11:e0154936.
104. Segev G, Yas-Natan E, Shlosberg A, Aroch I (2006): Alpha-chloralose poisoning in dogs and cats: A retrospective study of 33 canine and 13 feline confirmed cases. Vet J 172:109–113.
105. Zhao F, Jin T, Wang P, Kim SG (2007): Isoflurane anesthesia effect in functional imaging studies. Neuroimage 38:3–4.
106. Leoni RF, Paiva FF, Henning EC, Nascimento GC, Tannús A, de Araujo DB, Silva AC (2011): Magnetic resonance imaging quantification of regional cerebral blood flow and cerebrovascular reactivity to carbon dioxide in normotensive and hypertensive rats. Neuroimage 58:75–81.
107. Kufahl PR, Pentkowski NS, Heintzelman K, Neisewander JL (2009): Cocaine-induced Fos expression is detectable in the frontal cortex and striatum of rats under isoflurane but not alpha-chloralose anesthesia: implications for FMRI. J Neurosci Methods 181:241–248.
108. Weber R, Ramos-Cabrer P, Wiedermann D, van Camp N, Hoehn M (2006): A fully noninvasive and robust experimental protocol for longitudinal fMRI studies in the rat. Neuroimage 29:1303–1310.
109. Hall JE, Uhrich TD, Barney JA, Arain SR, Ebert TJ (2000): Sedative, amnestic, and analgesic properties of small-dose dexmedetomidine infusions. Anesth Analg 90:699–705.
110. King PR, Gundlach AL, Louis WJ (1995): Quantitative autoradiographic localization in rat brain of alpha 2-adrenergic and non-adrenergic I-receptor binding sites labelled by [3H]rilmenidine. Brain Res 675:264–278.
111. Nasrallah FA, Tan J, Chuang KH (2012): Pharmacological modulation of functional connectivity: α2-Adrenergic receptor agonist alters synchrony but not neural activation. Neuroimage 60:436–446.

112. Fukuda M, Vazquez AL, Zong X, Kim SG (2013): Effects of the α_2-adrenergic receptor agonist dexmedetomidine on neural, vascular and BOLD fMRI responses in the somatosensory cortex. Eur J Neurosci 37:80–95.
113. Schwarz AJ, Gass N, Sartorius A, Risterucci C, Spedding M, Schenker E, *et al.* (2013): Anti-correlated cortical networks of intrinsic connectivity in the rat brain. Brain Connect 3:503–511.
114. Pawela CP, Biswal BB, Hudetz AG, Schulte ML, Li R, Jones SR, *et al.* (2009): A protocol for use of medetomidine anesthesia in rats for extended studies using task-induced BOLD contrast and resting-state functional connectivity. Neuroimage 46:1137–1147.
115. Aantaa R, Kanto J, Scheinin M, Kallio A, Scheinin H (1990): Dexmedetomidine, an alpha 2-adrenoceptor agonist, reduces anesthetic requirements for patients undergoing minor gynecologic surgery. Anesthesiology 73:230–235.
116. Scheinin H, Virtanen R, Macdonald E, Lammintausta R, Scheinin M (1989): Medetomidine—a novel α2-adrenoceptor agonist: A review of its pharmacodynamic effects. Prog Neuropsychopharmacol Biol Psychiatry 13:635–651.
117. Aantaa R, Jaakola ML, Kallio A, Kanto J (1997): Reduction of the minimum alveolar concentration of isoflurane by dexmedetomidine. Anesthesiology 86:1055–1060.
118. Kallio A, Salonen M, Forssell H, Scheinin H, Scheinin M, Tuominen J (1990): Medetomidine premedication in dental surgery—a double-blind cross-over study with a new alpha 2-adrenoceptor agonist. Acta Anaesthesiol Scand 34:171–175.
119. Brynildsen JK, Hsu LM, Ross TJ, Stein EA, Yang Y, Lu H (2017): Physiological characterization of a robust survival rodent fMRI method. Magn Reson Imaging 35:54–60.
120. Grandjean J, Schroeter A, Batata I, Rudin M (2014): Optimization of anesthesia protocol for resting-state fMRI in mice based on differential effects of anesthetics on functional connectivity patterns. Neuroimage 102(Pt 2):838–847.
121. Zhao F, Holahan MA, Houghton AK, Hargreaves R, Evelhoch JL, Winkelmann CT, Williams DS (2015): Functional imaging of olfaction by CBV fMRI in monkeys: Insight into the role of olfactory bulb in habituation. Neuroimage 106:364–372.
122. Liang X, Hsu LM, Lu H, Sumiyoshi A, He Y, Yang Y (2018): The rich-club organization in rat functional brain network to balance between communication cost and efficiency. Cereb Cortex 28:924–935.
123. Liang Z, Li T, King J, Zhang N (2013): Mapping thalamocortical networks in rat brain using resting-state functional connectivity. Neuroimage 83:237–244.
124. Bertero A, Liska A, Pagani M, Parolisi R, Masferrer ME, Gritti M, *et al.* (2018): Autism-associated 16p11.2 microdeletion impairs prefrontal functional connectivity in mouse and human. Brain 141:2055–2065.
125. Sforazzini F, Schwarz AJ, Galbusera A, Bifone A, Gozzi A (2014): Distributed BOLD and CBV-weighted resting-state networks in the mouse brain. Neuroimage 87:403–415.
126. Greicius M (2008): Resting-state functional connectivity in neuropsychiatric disorders. Curr Opin Neurol 21:424–430.
127. Greicius MD, Srivastava G, Reiss AL, Menon V (2004): Default-mode network activity distinguishes Alzheimer's disease from healthy aging: Evidence from functional MRI. Proc Natl Acad Sci U S A 101:4637–4642.
128. Lustig C, Snyder AZ, Bhakta M, O'Brien KC, McAvoy M, Raichle ME, *et al.* (2003): Functional deactivations: Change with age and dementia of the Alzheimer type. Proc Natl Acad Sci U S A 100:14504–14509.
129. Gu H, Salmeron BJ, Ross TJ, Geng X, Zhan W, Stein EA, Yang Y (2010): Mesocorticolimbic circuits are impaired in chronic cocaine users as demonstrated by resting-state functional connectivity. Neuroimage 53:593–601.
130. Ma N, Liu Y, Li N, Wang CX, Zhang H, Jiang XF, *et al.* (2010): Addiction related alteration in resting-state brain connectivity. Neuroimage 49:738–744.
131. Sutherland MT, McHugh MJ, Pariyadath V, Stein EA (2012): Resting state functional connectivity in addiction: Lessons learned and a road ahead. Neuroimage 62:2281–2295.
132. Ritter P, Villringer A (2006): Simultaneous EEG-fMRI. Neurosci Biobehav Rev 30:823–838.
133. Liu Z, Ding L, He B (2006): Integration of EEG/MEG with MRI and fMRI. IEEE Eng Med Biol Mag 25:46–53.
134. de Pasquale F, Della Penna S, Snyder AZ, Marzetti L, Pizzella V, Romani GL, Corbetta M (2012): A cortical core for dynamic integration of functional networks in the resting human brain. Neuron 74:753–764.
135. Horovitz SG, Fukunaga M, de Zwart JA, van Gelderen P, Fulton SC, Balkin TJ, Duyn JH (2008): Low frequency BOLD fluctuations during resting wakefulness and light sleep: A simultaneous EEG-fMRI study. Hum Brain Mapp 29:671–682.
136. Wang L, Saalmann YB, Pinsk MA, Arcaro MJ, Kastner S (2012): Electrophysiological low-frequency coherence and cross-frequency coupling contribute to BOLD connectivity. Neuron 76:1010–1020.
137. Pan W, Thompson G, Magnuson M, Jaeger D, Keilholz S (2013): Infraslow LFP correlates to resting-state fMRI BOLD signals. Neuroimage 74:288–297.
138. Magri C, Schridde U, Murayama Y, Panzeri S, Logothetis NK (2012): The amplitude and timing of the BOLD signal reflects the relationship between local field potential power at different frequencies. J Neurosci 32:1395–1407.
139. Fox KCR, Foster BL, Kucyi A, Daitch AL, Parvizi J (2018): Intracranial electrophysiology of the human default network. Trends Cogn Sci 22:307–324.
140. Lu H, Stein E (2014): Resting state functional connectivity: Its physiological basis and application in neuropharmacology. Neuropharmacology 84:79–89.
141. Voorn P, Vanderschuren LJMJ, Groenewegen HJ, Robbins TW, Pennartz CMA (2004): Putting a spin on the dorsal-ventral divide of the striatum. Trends Neurosci 27:468–474.
142. Karreman M, Westerink BH, Moghaddam B (1996): Excitatory amino acid receptors in the ventral tegmental area regulate dopamine release in the ventral striatum. J Neurochem 67:601–607.
143. Hutchison R, Hashemi N, Gati J, Menon R, Everling S (2015): Electrophysiological signatures of spontaneous BOLD fluctuations in macaque prefrontal cortex. Neuroimage 113:257–267.
144. Winder AT, Echagarruga C, Zhang Q, Drew PJ (2017): Weak correlations between hemodynamic signals and ongoing neural activity during the resting state. Nat Neurosci 20:1761–1769.
145. Mateo C, Knutsen PM, Tsai PS, Shih AY, Kleinfeld D (2017): Entrainment of arteriole vasomotor fluctuations by neural activity is a basis of blood-oxygenation-level-dependent "resting-state" connectivity. Neuron 96:936–948.e3.
146. Ma Y, Shaik MA, Kozberg MG, Kim SH, Portes JP, Timerman D, Hillman EMC (2016): Resting-state hemodynamics are spatiotemporally coupled to synchronized and symmetric neural activity in excitatory neurons. Proc Natl Acad Sci U S A 113:E8463–E8471.
147. Matsui T, Tamura K, Koyano KW, Takeuchi D, Adachi Y, Osada T, Miyashita Y (2011): Direct comparison of spontaneous functional connectivity and effective connectivity measured by intracortical microstimulation: An fMRI study in macaque monkeys. Cereb Cortex 21:2348–2356.
148. Steinmetz NA, Buetfering C, Lecoq J, Lee CR, Peters AJ, Jacobs EAK, *et al.* (2017): Aberrant cortical activity in multiple GCaMP6-expressing transgenic mouse lines. eNeuro Sep 6;4(5).
149. Lu H, Yang Y, Stein EA (2015): Systems and methods for training and imaging an animal in an awaken state. Available at: https://patents.google.com/patent/US20160192891A1/en. Accessed April 17, 2018.
150. Lu H, Cover C, Kesner A, Stein E, Ikemoto S, Yang Y (2018): A novel approach for fMRI of rodents actively performing optogenetic self-stimulation. Proceedings of the International Society of Magnetic Resonance in Medicine Annual Meeting, June 16–21, Paris, France, p 1212.
151. Lu H, Wang L, Rea WW, Brynildsen JK, Jaime S, Zuo Y, *et al.* (2016): Low- but not high-frequency LFP correlates with spontaneous BOLD fluctuations in rat whisker barrel cortex. Cereb Cortex 26:683–694.